Routes To Development Of Near-Surface Alloy Composition Anomaly[1]

Y. W. Kim[2]

Thermophysical data in the literature for metallic alloys, including single-element specimens, exhibit a high degree of variability. Of interest is if the reasons are intrinsic. That there exists as a rule a surface layer whose elemental composition differs from that of the bulk has been demonstrated. Such a near-surface composition anomaly can, in principle, account for the significant part of the variability. The method of time-resolved spectroscopy of emissions from laser-produced plasma (LPP) plumes has been the key in this new development because both the elemental composition and thermal diffusivity can be measured simultaneously. Multiple application of LPP analysis leads to depth-resolved measurements. A variety of alloy specimens have been subjected to different scenarios of thermal cycling to find that thermal cycling modifies the near-surface composition profile of a given specimen. A new study has been carried out with Wood's alloy as a model system by forcing the specimen into melting at increasing temperature. This investigation has revealed that the near-surface composition undergoes sharp irreversible changes when the highest elemental melting point has been exceeded before the specimen is cooled to resolidification. A possible mechanism is suggested.

KEY WORDS: alloy composition anomaly; laser-produced plasma; thermal cycling; thermal diffusivity; Wood's alloy.

1. INTRODUCTION

A question of significant interest from the standpoint of thermophysical property measurement is how representative the surface of a material specimen is of its bulk in elemental composition. This is because in the great

---

[1]Paper presented at the Seventh International Workshop on Subsecond Thermophysics, October 6–8, 2004, Orléans, France

[2]Department of Physics, Lewis Laboratory #16, Lehigh University, Bethlehem, Pennsylvania 18015-3182, U.S.A. E-mail: ywk0@lehigh.edu

majority of thermophysical property measurement activities the primary sensors make contact with the specimen's surface. The contact may be of optical, electrical, or other physical character. The outputs of such sensors are dominated by the near-surface properties as dictated by the local elemental composition. With development of the method of laser-produced plasma (LPP) plume spectroscopy, certain thermophysical property measurements can now be carried out simultaneously with elemental composition determination. Some of the results from the LPP plume studies have been both surprising and revealing. For many multi-element alloy specimens, elemental composition profiles have been found to be depth-dependent in that the near surface composition is significantly different from the bulk composition [1–3]. It is self evident that such composition non-uniformity adversely affects the measurement of basic material properties in alloys. It also leaves the certainty of some of the basic thermophysical data open to interpretation in the presence of significant variability in the literature data.

Manufacturing of alloys and subsequent fabrication of material specimens entail a clearly complex sequence of processing steps. From the standpoint of the measurement community, the fact that these steps are often unspecified, unknown, and not standardized presents a serious quandary. Successful studies include a variety of metallic alloys, solid as well as molten, ranging from stainless steel alloys [4, 5], galvanized steel [6], Nichrome [7], magnetic mu-metal [8], Wood′s alloy [8], to titanium thin film on a copper substrate [9]. The profiles of both the elemental composition and thermophysical properties were found to change as the thermal state of the specimen evolves over time.

We now know that the depth-dependent near-surface composition profile is a direct outcome of the history of materials processing and thermo-mechanical treatments. The history is highly variable, and the development of an elemental composition profile and a specimen's morphology appears to be sensitively affected by the details of the history.

In this paper we present a continuing study of the effects of thermal cycling on the dynamics of the depth-resolved elemental composition profile. Wood's alloy, a low melting-point metallic alloy, is used as a model system for this study. Specifically, the Wood's alloy specimen used is composed of 50 mass% bismuth, 25 mass% lead, 12.5 mass% tin, and 12.5 mass% cadmium.

The study is carried out by using the method of time-resolved spectroscopy of the emissions from the LPP plume of a sub-micron surface layer of the specimen. It allows simultaneous measurement of both the composition [1, 2] and thermal diffusivity of the surface layer [3, 8, 9]. Repetitive LPP excitations expose the depth dependence with 10-nm depth resolution.

2. EXPERIMENTAL ARRANGEMENT

The experimental arrangement for this study was described in a recent paper [11]. It consists of a quartz vacuum chamber, which is arranged vertically to accommodate melting of the specimen, and a system of optics which delivers the laser pulse from a Q-switched Nd:YAG laser to the specimen surface vertically from above and collects emissions from the LPP plume. The plume is imaged onto a spectrograph equipped with a gated intensified CCD detector. The laser pulse has the total energy set at 0.175 J and a full width at half maximum of 25 ns.

The crucible containing the Wood's alloy specimen is a cylindrical cup made of stainless steel 304 with 12.5-mm outer diameter. A replaceable Pyrex lining is added within the cup giving inside dimensions of 9 mm in diameter and 5 mm in depth. The crucible assembly is supported and heated by a Nichrome heater ribbon. The specimen temperature is measured over the range of room temperature to 400 °C by means of an alumel-chromel thermocouple attached to the exterior surface of the stainless steel cup.

The specimen chamber was first evacuated to better than 8×10^{-6} Torr (1.07×10^{-3} Pa) and then filled with pure argon to 150 Torr (or 2.00×10^{4} Pa) before forcing a specimen into thermal cycling. The chamber's top end is closed with a quartz lens, which focuses the incoming laser pulse and collects the emissions from the LPP plume for spectroscopy. A high-power dichroic mirror located above the lens separates the laser beam from the plume emissions.

3. EXPERIMENTAL PROTOCOL

The LPP analysis method exploits the fact that at sufficiently high laser power density the advancing front of surface ablation moves in pace with the thermal diffusion front. Under such conditions, material ablation proceeds independently of the rate of evaporation that is normally element specific. The result is a LPP plume whose elemental composition is the same as in the bulk of the target specimen. The LPP plume is so high in particle number density that the mean particle collision time is of the order of 10 fs, and thus remains in local thermodynamic equilibrium for the dynamics that evolves with nanosecond time scales. Since the distance traveled by the thermal diffusion front governs the laser ablation, it is possible to determine the thermal diffusivity of the target specimen once the mass loss has been measured [3]. The mass loss can be measured by spectroscopic analysis of the LPP plume emissions.

The ultimate ablative thickness loss is a result of the competition among three materials properties: the local thermal diffusivity, heat of for-

mation required for ablation, and the diffusive dispersal of the atomic species entrained into the LPP plume. This has been codified in the form of a scaling relation:

$$\theta = C D_T^\alpha M^\beta H_f^\gamma. \tag{1}$$

Here θ denotes the thickness in cm, D_T is the thermal diffusivity in units of $cm^2 \cdot s^{-1}$, M is the molar mass, and H_f is the heat of formation in $J \cdot g^{-1}$. We have determined by experiment that $\alpha = 0.91 \pm 0.01$, $\beta = -\alpha$, and $\gamma = -1$. C depends on the laser power and pulse shape properties and the size of the surface area at the target specimen but it is independent of the materials being studied. For a two-joule Q-switched Nd-glass laser pulse of 20-ns FWHM, we have found that $C = 11.07 \pm 0.45$, when the laser pulse is diffusely focussed on a 2.5-mm diameter surface area of the target specimen in a vacuum. The scaling relation is most conveniently used to determine the thermal diffusivity relative to that of a reference, such as the value of the bulk matter, deep in the interior of the specimen. For alloys, M, H_f, and D_T take on the values for the alloy specimen given by the sum of the respective elemental values weighted according to elemental mass% values

Against this background, we focus on the evolution of the elemental composition profile as precipitated by different regimens of thermal cycling applied to the Wood's alloy specimens.

Two separate Wood's alloy specimens were used in this study. Specimen I was prepared by applying three consecutive cycles of heating and cooling. It was first heated to 152°C, cooled to 29°C, heated to 204°C, cooled to 153°C, heated again for the third time to 371°C, and was finally cooled for LPP analysis runs. Some aspect of the study with this specimen was reported earlier [11].

In order to shed light on the processes of composition profile modification, the second fresh specimen (Specimen II-a) was heated to melting at 204°C and cooled to room temperature. Specimen II-a has been analyzed for near-surface composition and mass loss per LPP pulse by carrying out 100 consecutive LPP analysis runs. The same specimen was then heated for the second time to melting at 260°C and cooled to room temperature (now Specimen II-b). A second round of 100 consecutive LPP analysis runs has been carried out on Specimen II-b.

4. MEASUREMENTS AND ANALYSIS

Each sequence of LPP measurement runs is prepared by carrying out calibration procedures for elemental abundance and mass loss determination. A fresh specimen of smooth surface is prepared by melting it at low

temperature (at just above the melting point of 71°C) and letting it solidify to a smooth surface finish. Altogether, five emission lines are used to deduce the composition and mass-loss values, one each for lead, tin, and bismuth, and two for cadmium.

A set of LPP plume emission spectra was taken to establish the quantitative relationship between the spectral emission line intensities and relative elemental abundance for each element, according to the manufacturer's composition specification. Here, the detected line intensities range from a few thousands to twenty thousands of photoelectrons, giving counting errors of 1 to 0.8%. The uniformity of elemental concentration is unknown other than by our own spectroscopic measurements, and therefore, there are no comparisons to be made against our measurements.

In addition, spectroscopic mass-loss measurement is calibrated as follows. The mass of the sample was first measured by using a digital microbalance, and it was remeasured after 300 LPP ablations had been administered in argon at 150 Torr in order to assign an absolute value for the mass loss per LPP shot. For the calibration sample we used, the mass loss was found to be 5.4 μg per LPP shot on average, which translates to 0.08 μm in thickness of the surface layer removed under the given experimental condition. The calibrated spectral intensities are summed for the entire sequence of 300 analysis runs, and this is compared with the measured total mass loss of the specimen to determine the absolute calibration constant for spectroscopic mass-loss determination.

In earlier studies of the near-surface composition anomaly issue [8, 10, 11], we have demonstrated the existence of a significant causal relationship between the thermal history of an alloy specimen and its near-surface composition profile. One such process of great relevance is the heating and cooling history, as typically encountered in the course of alloy refinement, melting, and solidification. As the thermal state of a given specimen is changed, the measured thermophysical properties change in response, but normally the changes are approximately reversible. We have discovered that under certain conditions the thermal history can lead to irreversible changes in the near-surface composition of the specimen with associated changes in the measured thermophysical properties. The case in point is the existence for the Wood's alloy specimens of a threshold temperature of about 335°C, such that heating beyond the threshold temperature drives the near-surface composition irreversibly away from its bulk composition.

The focus of the present study is to shed light on the detail of both the process and the elemental composition structure of the near-surface layers of the Wood's alloy specimen that have the above-threshold heating history.

Figure 1 compares the depth-resolved elemental compositions for Wood's alloy specimens having three different thermal histories. Results are organized according to increasing complexity of the thermal history of specimens. In Fig. 1(a), the element-resolved concentration (in mass%) data are shown as a function of increasing shot number of LPP runs for a fresh Wood's alloy specimen (Specimen II-a) after it has been heated once to 204°C and cooled to room temperature. The results of 100 consecutive analysis runs are shown, probing successively deeper into the bulk. Figure 1(b) shows the data for Specimen II-b, which is Specimen II-a of Fig. 1(a) after heating a second time to a higher temperature of 260°C. Again, 100 LPP analyses were carried out. In Fig. 1(c), we show the element-resolved mass loss per LPP pulse data for Specimen I. This specimen has been thermally cycled according to the following schedule: heated to 152°C, cooled to 29°C, heated to 204°C, cooled to 153°C, and heated again to 371°C and cooled.

Depth-resolved mass loss and elemental composition data for Specimen I are shown in Fig. 2. Altogether 300 consecutive LPP analysis runs have been carried out. Figure 3 shows the results of the Specimen I analysis in the form of element resolved mass loss per LPP pulse as a function of depth from the free surface of the specimen at the start of the analyses. The elemental mass loss in Fig. 3 shows a depression for all elements in the depth range of 5–9 μm from the free surface. The exact reasons are unknown. It is possible that it might signify a transition from the layer that is dominated by the surface effects to the region controlled by the bulk properties. The heating, especially beyond the highest elemental melting point, may have increased the size in depth of the surface zone.

A comparison of the results shown in Fig. 1 suggests the following physical picture. Melting of the specimen by modest heating followed by re-solidification by cooling results in modest changes of the near-surface composition profile. Each successive heating–cooling cycle applied to a single specimen has a cumulative effect on the specimen's near-surface composition profile. These benign trends make a drastic turn when the heating cycle includes heating in excess of a threshold temperature. Specifically, the heating history of Specimen I includes the specimen temperature exceeding the threshold temperature at about 335°C. The near-surface composition is characterized by a sharply increased concentration of cadmium relative to bismuth. Attempts to reverse the cadmium domination in the near-surface composition profile by further heating have not been successful, indicating that the near-surface composition profile is irreversibly changed.

The measurement errors are small. The uncertainty in the specimen temperature measurement is due mainly to reading error and a small thermal gradient across the crucible containing the molten alloy pool and is
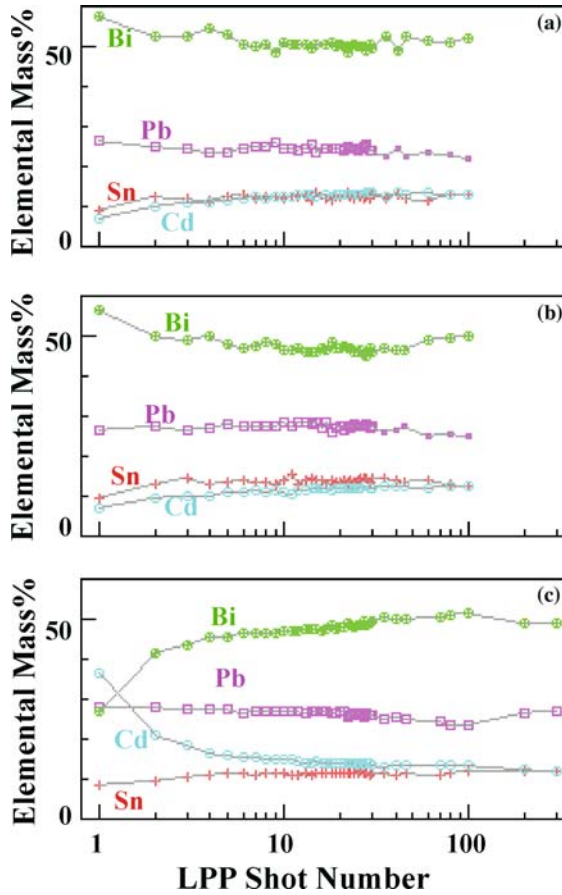
Fig. 1. Measured elemental concentration in mass% versus LPP shot number for three different thermally cycled Wood's alloy specimens. (a) Shows the measurements for Specimen II-a, a fresh specimen that has been heated once to 204°C and cooled to room temperature; (b) shows the results for Specimen II-b, the specimen of (a) after heating for the second time to 260°C and cooling to room temperature; (c) Summarizes the results of 300 LPP analyses for Specimen I, a fresh specimen that has been heated and cooled three consecutive times (see the text description for the thermal cycling protocol in this paper and in Ref. 11).
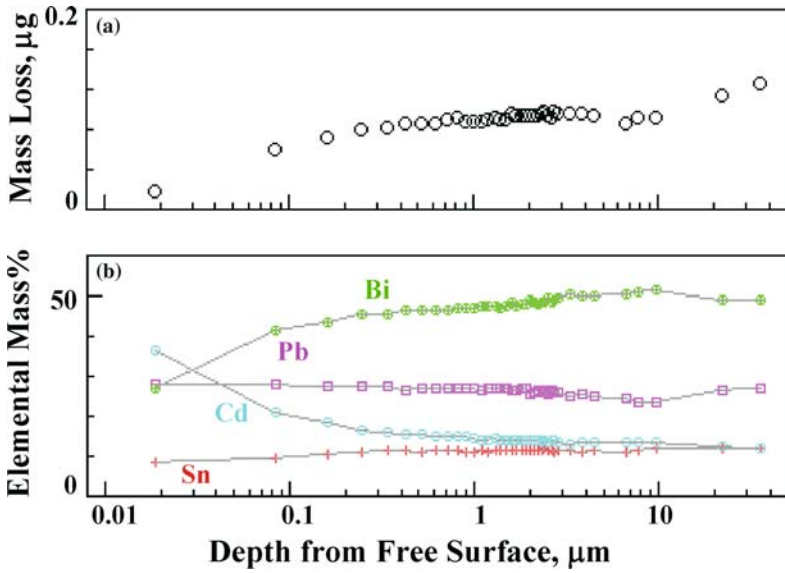
Fig. 2. (a) Measured mass loss per LPP pulse and (b) elemental concentration in mass% for Specimen I are plotted as a function of depth from the specimen's free surface.
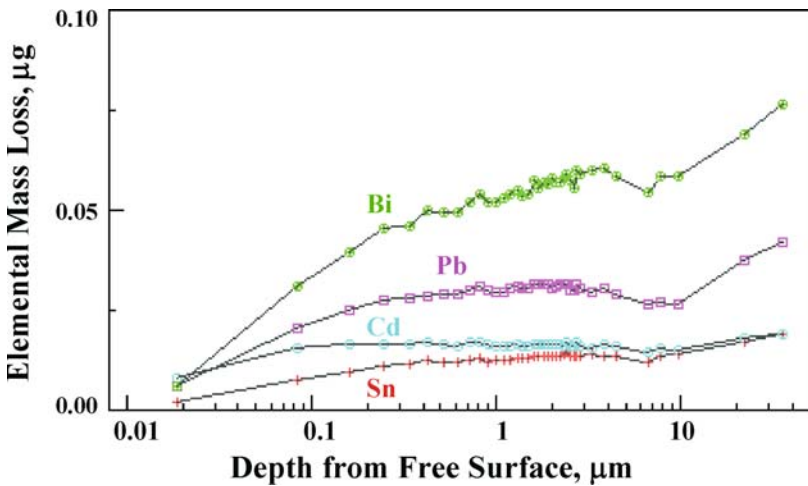

Fig. 3. Element-resolved mass loss per LPP pulse for Specimen I is plotted as a function of depth from the specimen's free surface.

estimated to be within $\pm 1°$C. The uncertainties in the measurements of the mass loss per LPP shot, elemental composition, and the thickness of the ablated layer stem from the photon counting statistics in the measurement of the spectral emission intensity. The strongest emission lines are employed for each of the four constituent elements. The number of detected photoelectrons is of the order of 1×10^4, which gives an intensity measurement uncertainty of 1% or less. The thermal noise contribution over the 390 ns integration time has been minimal because the CCD detector has been cooled to $0°$C by a Peltier cooler.

Conversion of the intensities to elemental masses relies on the manufacturer's composition specification and the measured cumulative mass loss by a fresh specimen due to 300 LPP ablations, and this has been determined to better than 1%. The overall uncertainty in determining the ablative loss in mass and in surface layer thickness as well as elemental composition is estimated to be less than 2%. These errors are smaller than the size of the symbols used to represent the data points in the figures.

5. CONCLUDING REMARKS

Using Wood's alloy specimens as a model alloy system, we have demonstrated the existence of a significant causal relationship between the thermal history of an alloy specimen and its near-surface composition profile. The central issue here has to do with the fact that many measured thermophysical properties of a given material specimen are strongly influenced by the near-surface elemental composition, while the near-surface composition can be driven away from the bulk composition by myriad processes of forcing applied to the specimen. These processes play different roles in the course of alloy refinement, melting, and re-solidification and in specimen preparation, and during storage. The interaction of the specimen with measurement instrumentation is affected by the changes in the near-surface composition profile and specimen morphology, thus influencing the eventual outcome of thermophysical property measurements.

One of the predominant processes is thermal cycling. The present study demonstrates that the thermal history's effect on the specimen's near-surface composition is modest but is cumulative. When the specimen temperature exceeds the threshold temperature, as defined by the highest melting point of the constituent elements, the movement of the near-surface composition profile undergoes a large, sudden, and irreversible change, at least, in the case of Wood's alloy. The threshold temperature for the Wood's alloy specimen is at about 335 $°$C, which is just above the melting point of lead, the highest melting point among the four constituent elements. In order to demonstrate the history dependence of the

near-surface composition profile, the present study has accentuated the causal relationship by forcing the Wood's alloy specimens through a wide range of thermal cycling. This, however, should not diminish the adverse effects the thermal history imposes on a specimen used in thermophysical property measurement activities.

The melting points of the constituent elements are: bismuth at 271.3°C (544.4 K), lead at 327.46°C (600.61 K), tin at 231.93°C (505.08 K), and cadmium at 321.07°C (594.22 K). The question is what is so particular about the highest melting point of the constituent elements of the alloy? If we view the near-surface composition as resulting from the cumulative transport of elements in the molten phase, the results of Fig. 3 reveal that the cadmium transport is de-coupled from that of bismuth when Specimen I is heated to a molten phase at 371°C. This is a distinctive departure from the patterns of transport by the same two elements in Specimens II-a and II-b that have been heated to lower temperatures. It may be possible to speculate that all of the constituent elements in the alloy become de-coupled from each other when the alloy is heated to above the highest elemental melting point, freeing the elemental atoms to fluctuate according to their respective intrinsic elemental properties. If so, they may diffuse in the presence of just the free surface and gravity, less restricted by the collective modes of the alloying matrix.

This hypothesis should have measurable consequences. One, the near-surface elemental composition profile of the type shown in Fig. 3 should reveal a dependence on the residence time of the specimen in such an above-threshold molten state. Two, the four-element alloy may eventually segregate into stratification by elements. We plan to examine the hypothesis experimentally.

A mechanism has been suggested in the literature for ordering of atoms into several planar layers near the free surface when a pure or binary alloy is in a molten state [12, 13], and these may freeze into a solid. The thickness of such a layer is much smaller than what our experiment shows, however.

We have considered the onset of Rayleigh–Benard convection within the melt. The basic data on Wood's alloy is only sketchy [14, 15], but we have concluded against it given the likelihood of high thermal conductivity and extremely large viscosity in the melt and a small thermal gradient across the specimen height. The data of Fig. 3 also appear counter to such a possibility.

REFERENCES

1. Y. W. Kim, in *Laser-Induced Plasmas and Applications*, L. J. Radziemski and D. A. Cremers, eds. (Marcell Dekker, New York, 1989). Chap. 8.
2. Y. W. Kim, *High Temp. Sci.* **26**:57 (1990).

3. Y. W. Kim, *Int. J. Thermophys.* **14**:397 (1993).
4. Y. W. Kim and C. -S. Park, *Int. J. Thermophys.* **17**:713 (1996).
5. Y. W. Kim and C. -S. Park, *Int. J. Thermophys.* **17**:1125 (1996).
6. Y. W. Kim, *Int. J. Thermophys.* **20**:1313 (1999).
7. Y. W. Kim, *Int. J. Thermophys.* **23**:1103 (2002).
8. Y. W. Kim, *Int. J. Thermophys.* **23**:1171 (2002).
9. Y. W. Kim, *Int. J. Thermophys.* **23**:1091 (2002).
10. Y. W. Kim, in *Thermal Conductivity 26*, R. B. Dinwiddie, ed. (DEStech Publications, Lancaster, Pennsylvania, 2005), pp. 146–158.
11. Y. W. Kim, *Int. J. Thermophys.* **25**:575 (2004).
12. H. Tostmann, E. DiMasi, O. G. Shpyrko, P. S. Pershan, B. M. Ocko, and M. Deutsch, *Ber. Bunsenges. Phys. Chem.* **102**:1136 (1998).
13. E. DiMasi, H. Tostmann, O. G. Shpyrk, M. Deutsch, P. S. Pershan, and B. M. Ocko, *J. Phys.: Condens. Matter* **12**:A209 (2000).
14. M. Lamvik and J. M. Zhou, *Meas. Sci. Technol.* **6**:880 (1995).
15. M. Iguchi and H. Tokunaga, *Metall. Meter. Trans. B* **33B**:695 (2002).